

0476

Morphing and Posing of Computational Anatomical Models: Enhanced Patient-Specific MRI RF Exposure Prediction

Manuel Murbach¹, Bryn A. Lloyd¹, Esra Neufeld¹, Wolfgang Kainz², and Niels Kuster^{1,3}¹ITIS Foundation, Zurich, Switzerland, ²US Food and Drug Administration (FDA), Silver Spring, MD, United States, ³ETH Zurich, Zurich, Switzerland

Synopsis

The current MRI safety standards for exposure to radiofrequency fields are conservative and intended to protect the entire patient population. Limits set on whole-body average specific absorption rate take the patient's weight into consideration, which allows robust, but only very rudimentary patient-specific exposure estimation. The introduction of combined morphing and posing in computational anatomical human models will enable further improvements in the accuracy of *in silico* local exposure estimation. In this study, we developed refined morphing techniques and explored the benefits for estimating personalized radiofrequency absorption, which could substantially reduce the safety margins necessary for conservative assessment of radiofrequency exposure.

Purpose

Magnetic resonance imaging (MRI) is a powerful non-invasive imaging technique. However, the amount of radiofrequency (RF) energy absorbed by the patient – expressed as the specific absorption rate (SAR) – must be carefully managed. *In silico* safety assessments are becoming increasingly important in both academic safety research and regulatory compliance certification processes.

Currently, a broad patient population with highly diverse body sizes and geometries profit from the use of MRI scanners. Computational anatomical human models – such as the Virtual Population 3.0 (ViP)¹ – allow *in silico* RF exposure estimation for a broad, but limited, patient population (Figure 1). Gross anatomical descriptors correlate with SAR, but the correlation becomes weak when normalized to whole-body average SAR due to localized individual anatomical variations and the postures of the models². Therefore, we have developed novel morphing and posing tools to improve population coverage by including more obese and underweight patients, as well as patients with varying local anatomies and postures. The obtained model-parameterization improves our understanding of absorption mechanisms and allows us to better estimate patient-specific personalized exposure by mapping an individual patient to a similar pre-computed model or model variant.

Methods

We have developed a technique for local or regional shrinkage or expansion of tissues, whereby the body is treated as a deformable hyper-elastic material with rigid bones. Specific tissues can be parametrized by locally prescribing initial strain^{3,4} thereby controlling the volume. The tissue deformation is constrained by the proximity of nearby rigid bones and regularized by the presence of surrounding soft tissue. The method is combined with an approach for changing the posture of anatomical models, whereby bones are moved by prescribed rotations around articulated joints. The bone hierarchy allows relative transforms to be propagated from a 'parent' bone to all 'child' bones, and the new bone positions are applied as constraints to the biomechanical finite element (FEM) simulation. An example showing combined morphing and posing of the ViP model ELLA is depicted in Figure 2.

Figure 3 shows an initial set of model-variants produced by morphing (FATS), posing (LOUIS and DUKE), and combined morphing and posing (FATS). All model-variants were simulated in the abdomen imaging position within a 3T body coil with circularly polarized excitation and were normalized to either a fixed B1 incidence field or to a whole-body SAR of 4 W/kg. The morphing process iteratively adds or removes fatty tissues, while ensuring continuity of structures like muscles and blood vessels (see Figure 3). As local SAR is highly dependent on the cross-section of the body, the models have been adjusted – where possible – to similar lateral body positioning (distance between the two arms). This allows for the first time to directly compare the influence of anatomical properties, i.e., the body mass index (BMI), to that of posture changes of the patient.

Results

The local RF exposure of FATS, morphed to different levels of obesity, increases with decreasing BMI (Figure 4). This finding is somewhat counterintuitive, as obese patients generally have higher local exposures², and needs to be investigated further; a possible explanation is that similar eddy currents must pass through a smaller conductive cross-section in the arms. More expected was the increase in local absorption as a function of arm-distance. The combined morphing and posing of FATS to achieve a BMI and arm-distance similar to those of DUKE leads to local SAR values within 20% of those for DUKE, which indicates that BMI and geometry may be key parameters for assessment of RF exposure. The deviating values found for 14-year-old LOUIS (Figure 4) – still under investigation – might be caused by age-related anatomical differences.

Conclusions

Conservative but not overly restrictive RF exposure safety assessment is essential for the effective and safe operation of MRI scanners to diagnose a broad patient population. Standard safety margins for MRI exposure could be reduced by considering the personalized exposure parameters of the actual patient, which would allow faster MRI scanning for most of the patient population. The combined morphing and posing techniques presented here provide unique insight into the RF exposure characteristics and allow identification of key-parameters with high impact on the exposure level. The technique can also be used to derive a patient-specific personalized exposure estimate via a generated library of reference models.

Disclaimer

The mention of commercial products, their sources, or their use in connection with material reported herein is not to be construed as either an actual or suggested endorsement of such products by the Department of Health and Human Services.

Acknowledgements

This work was supported in part by the MRI# project

References

1. Gosselin M-C, Neufeld E, Moser H, et al. Development of a new generation of high-resolution anatomical models for medical device evaluation: the Virtual Population 3.0. *Phys Med Biol* 2014;59:5287–5303.

2. Murbach M, Neufeld E, Kainz W, Pruessmann KP, Kuster N. Whole-body and local RF absorption in human models as a function of anatomy and position within 1.5T MR body coil. *Magn Reson Med* 2014;71:839-845.
3. Szczerba D, Neufeld E, Zefferer M, Bühlmann B, Kuster N. FEM based morphing of whole body human models. 2011 30th URSI General Assembly and Scientific Symposium, URSIGASS 2011 2011.
4. Lloyd BA. *Covering Population Variability: Morphing of Computation Anatomical Models*. International Workshop on Simulation and Synthesis in Medical Imaging. Springer International Publishing. 2016.
5. Ogden CL, Carroll MD, Kit BK, Flegal KM. Prevalence of childhood and adult obesity in the United States, 2011-2012. *J Amer Med Assoc* 2014;311:806-814.
6. Ogden CL, Fryar CD, Carroll MD, Flegal KM. Mean body weight, height, and body mass index, United States 1960-2002. *Advance data* 2004:1-17.
7. Growth Charts. National Center for Health Statistics in collaboration with the National Center for Chronic Disease Prevention and Health Promotion (2000). www.cdc.gov/growthcharts.

Figures

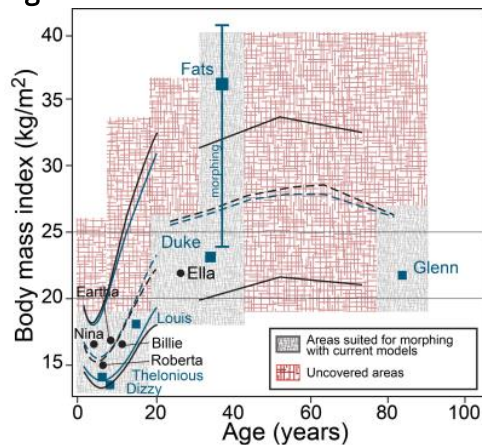


Figure 1: Comparison of the BMIs of the VIP models (males: blue squares; females: black circles), with age-dependent statistical data from ⁵⁻⁷; dashed lines: 50th percentile; solid lines: 5th and 95th percentiles. Through morphing, additional areas can be covered. The range of morphing applied for FATS is indicated.

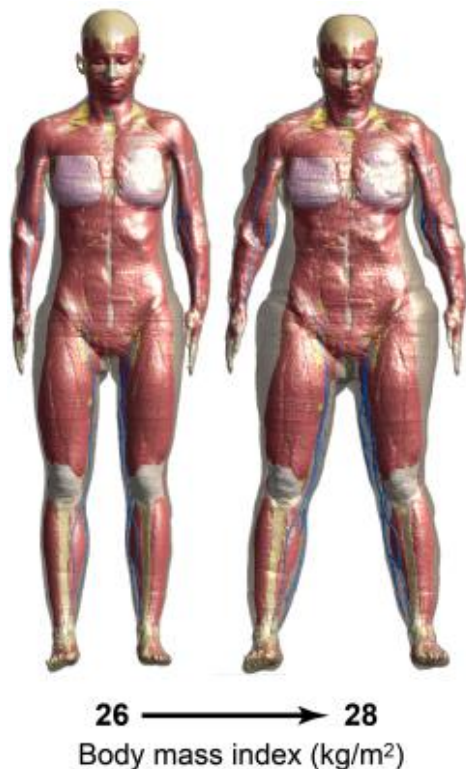


Figure 2: Anatomical model ELLA morphed and posed from the original shape with a BMI of 26 to a wider variant with a BMI of 28.

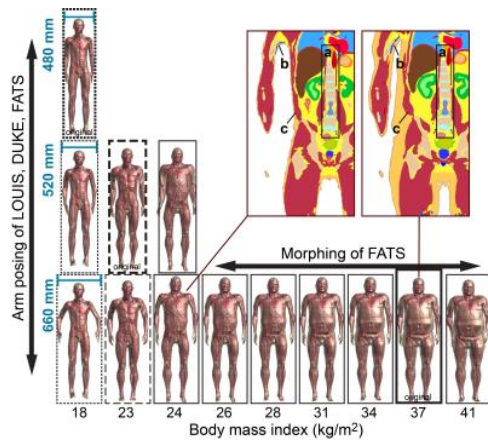


Figure 3: Initial set of model variations based on morphing of FATS (depicted within black boxes) to vary the BMI from 24 to 41. Two cross-sectional slice-views taken from the 24 and 37 BMI variants show a) the unchanged structure around non-movable bones, b) the continuity of vessels (vein in blue), and c) the reduced fat-content and altered muscle shape. Vertically, the distance between the arms is set to 480, 520, and 660 mm. The LOUIS model is depicted within dotted boxes, DUKE within dashed boxes.

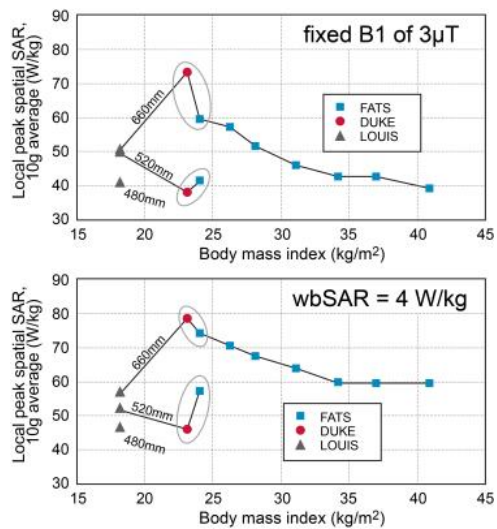


Figure 4: Local SAR (peak spatial SAR averaged over 10g tissue) for the model-variants shown in Figure 3, with normalization to a fixed B1 field of $3\mu\text{T}$ at the isocenter (top) and to a $\text{wbSAR} = 4 \text{ W/kg}$ (bottom). Reducing the BMI for FATS down to 24 results in local SAR values up to 25% higher. The SAR values of DUKE are similar to those of FATS when posed with the same distance between the arms (circled values), indicating that BMI and arm-distance may be key-parameters in RF absorption. For LOUIS, the arm-distance-dependent difference in SAR-variation appears to be lower.